ACS APPLIED MATERIALS & INTERFACES

Research Article

www.acsami.org

Random Terpolymer Designed with Tunable Fluorescence Lifetime for Efficient Organic/Inorganic Hybrid Solar Cells

Qinghua Li,[†,‡,§] Xiao Jin,[†,‡,§] Yinglin Song,[⊥] Qin Zhang,[§] Zhongyuan Xu,[§] Zihan Chen,[∥] Yuanyuan Cheng,[‡] and Xubiao Luo*[,‡]

[‡]Key Laboratory of Jiangxi Province for Persistent Pollutants Control and Resources Recycle and [§]Jiangxi Engineering Laboratory for Optoelectronics Testing Technology, Nanchang Hangkong University, Nanchang 330063, P. R. China

[⊥]Department of Physics, Harbin Institute of Technology, Harbin 150001, P. R. China

[∥]School of Photovoltaic and Renewable Energy Engineering, University of New South Wales, Sydney, New South Wales 2052, Australia

ABSTRACT: The long photoluminescence lifetime of the organic semiconductor materials is of great importance in assuring the photoexcited extion to have enough time to achieve successful separation at the interface and improving the performances of organic/inorganic hybrid solar cells. Unfortunately, many efforts have been devoted to the bandgap or molecular energy level control, whereas this viewpoint is rarely referred. Herein, we prepare a random D−A terpolymers based on PZT and BDT cores in conjugation with electron withdrawing BT unit and explore their applications in HSCs. Except for the energy level and the bandgap, the role that monomers ratio plays in photoluminescence lifetime is particularly involved. As a result, the average PL lifetimes of the terpolymer are significantly tuned. The optimized terpolymer exhibits a longer PL lifetime and prominent charge transfer ability, thus leading to a notable enhancement of PCE when compared with its counterparts, although their bandgaps and molecular energy levels are almost the same.

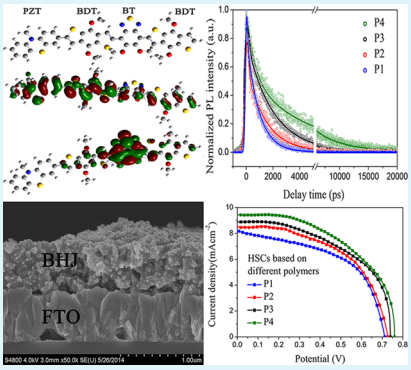

KEYWORDS: *organic/inorganic hybrid solar cell, random terpolymer, charge photogeneration dynamics, fluorescence lifetime, phenothiazine*

1. INTRODUCTION

Utilization of solar light is a promising way to meet the increasing energy consumption demands of the 21st century and a solution to global warming, ecological destruction, and fossil fuel depletion.[1] To this end, organic/inorganic hybrid solar cells (HSCs) have emerged and attracted prominent attention because of their unique advantages such as low production cost, low-temperature processing of the organic semiconductors, and high charge mobility of the inorganic ones.[2−4] Up to now, despite the developments of HSCs in recent years, their power conversion efficiencies (PCEs) have still been low, mostly ranging from 1 to 3%.[5−10]

Previously, many attempts had been devoted to narrow band gap polymers for the enhanced light harvest.[11,12] However, these demonstrations usually result in a low photoexcited carrier transfer efficiency, because suitable polymeric materials that have long lifetimes of the high lying excited state are not well deployed.[13] From the photovoltaic materials point of view, an ideal organic semiconductor requires a narrow band gap to ensure efficient light harvest from ultraviolet (UV) to near-infrared (NIR) spectrum, but also needs a long enough lifetime of the exitons to ensure the sufficient charge separation at the organic−inorganic interface.[14] Unfortunately, the lifetimes of the high-lying excited state are short in most of the existing organic semiconductors, thus resulting in poor photovoltaic performances. For example, poly(3-hexylthiophene) (P3HT) possesses a narrow band gap, i.e., ∼1.9 eV, which guarantees the competent solar light harvest (∼40%).[15] However, its singlet excited state lifetime is fairly short, typically within 2 ns,[16−18] thus leading to an insufficient photoexcited charge separation in the bulk heterojunction. Despite recent developments in organic/inorganic solar cells, these devices are still in infancy, and most of their PCEs are within 3%.[19−21]

An ideal polymer architecture should simultaneously have a low bandgap together with long exiton lifetime for PV applications. Donor−acceptor (D−A) alternating copolymers that comprises electron-rich (donor) and electron-deficient (acceptor) moieties have attracted increasing attention, owing to their virtually infinite and much wider possibilities for tunable electronic activities and absorption band edges.[22,23]Among the various conjugated copolymers, donor−acceptor (D−A) copolymers based on 2,1,3-benzothiadiazole (BT) acceptor with wide variety of donors such as derivatives of phenothiazine (PTZ) and benzo[1,2-b:4,5-b′]dithiophene (BDT) have already been perused for various photovoltaic applications.[24−26] As a heterocyclic compound with electron-

Received: May 29, 2015
Accepted: July 21, 2015
Published: July 21, 2015

DOI: 10.1021/acsami.5b04697
ACS Appl. Mater. Interfaces 2015, 7, 17408−17415

Scheme 1. Synthetic Route for Terpolymers

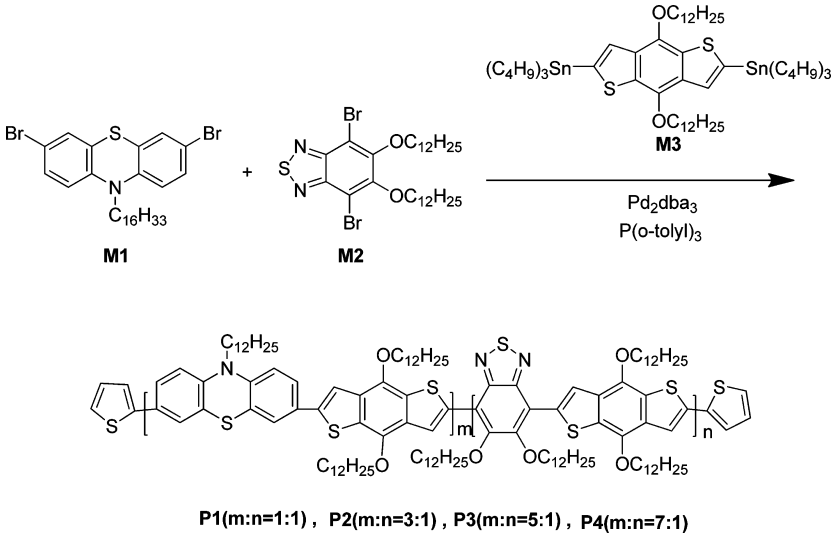

rich sulfur and nitrogen atoms, phenothiazine is proved to be a promising candidate in designing new copolymers to obtain high intramolecular charge transfer (ICT) abilities, because of its "butterfly" nonplanar geometry, which can impede π-stacking congestion, achieving low cost and good solubility by introducing solubilizing units.[27−29] Besides, planar benzodithiophene (BDT) donor units also have been utilized to achieve smaller band gaps, deeper highest occupied molecular orbital (HOMO) levels, and much more facile charge separation for PV applications.[30,31] Although electron withdrawing 2,1,3-benzothiadiazole (BT) have achieved extraordinary success in PV devices, where larger open voltage and higher stability are reached.[32] In addition, BT-based copolymers on one hand possess powerful electron-withdrawing ability because of its electron-deficient lactam rings, which can induce strong $\pi-\pi$ interactions. On the other hand, their relatively simple, symmetric, and planar structures guarantee the ease of fabrication.

Recently, random terpolymers with different donor and acceptor units have been explored.[24,33,34] These terpolymers can bring about synergistic effects on the boost of device performances, such as broadening the solar light absorption, enhancing charge generation and the subsequent transport. Terpolymers that incorporated with different electron-rich monomers are of particular interest to achieve broader solar light harvest, owing to the synergetic electron-pushing effects of the electron-donating units. The light absorption band could be broadened by the two individual electron-rich units which have the complementary light harvest range. Furthermore, the electronic behaviors of the polymers could be tuned by changing the donor units. Herein, we report the synthesis of new random D−A terpolymers based on the PZT and BDT cores in conjugation with electron withdrawing BT unit and their applications in HSCs. However, unlike other researches that mainly focus on pursuing small bandgap polymers, herein we investigate the effects of the monomer ratios on the singlet excited state lifetime and the final device performance in detail. By optimizing monomer ratios, a long PL lifetime of the terpolymer is obtained, thus leading to the device efficiency up to 3.72%.

2. EXPERIMENTAL SECTION

Characterization. The instruments for characterizing the nuclear magnetic resonance (NMR) spectra, cyclic voltammetry (CV), field emission scanning electron microscope (FE-SEM), photoluminescence (PL) spectra, UV−vis spectra and thermogravimetric analyses (TGA) and photocurrent−voltage ($J-V$) were used the same as our previous work.[35] Time-resolved photoluminescence (PL) were carried out by using a femtosecond pump setup at 400 nm wavelength, the fluorescent light was directed to a spectrometer (Bruker Optics 250IS/SM) and detected by an intensified charge coupled device detector (Andor, IStar740) with time resolution of ~60 ps.

Synthesis of 3,7-Dibromo-10-hexadecyl-10H-phenothiazine (M1). M1 was synthesized according to literature.[36] ^{1}H NMR($CDCl_3$, 400 Hz, δ/ppm): 7.18 (t, 4H), 6.63 (d, 2H), 3.71 (t, 2H), 1.71 (t, 2H), 1.36−1.22 (m, 26H), 0.87 (t, 3H). ^{13}C NMR($CDCl_3$, 100 MHz, δ/ppm): 144.1, 130.1, 129.6, 126.4, 116.6, 114.7, 47.6, 31.9, 29.7, 29.6, 29.5, 29.4, 29.1, 26.8, 26.6, 22.7, 14.1.

Synthesis of 4,7-Dibromo-5,6-bis(dodecyloxy)benzo[c]-[1,2,5] thiadiazole (M2). M2 was synthesized according to literature.[37] ^{1}H NMR ($CDCl_3$, 400 Hz, δ/ppm): 4.13−4.17(t, 4H), 1.83−1.90(t, 4H), 1.50−1.52 (t, 4H), 1.27(s, 32H), 0.86−0.89(m, 6H). ^{13}C NMR ($CDCl_3$, 100 MHz, δ/ppm): 155.68, 147.46, 99.59, 75.42, 31.94, 30.20, 29.69, 29.66, 29.63, 29.60, 29.38, 25.91, 22.71, 14.13.

Synthesis of 2,6-Bis(tributyltin)-4,8-didodecyloxybenzo[1,2-b; 3,4-b]dithiophene (M3). M3 was prepared by following the procedures in literature.[38] ^{1}H NMR ($CDCl_3$, 400 Hz, δ/ppm): 7.48 (s, 2H), 4.30 (t, 4H), 1.90−1.84(m, 4H), 1.66−1.58 (m, 12H), 1.41−1.27 (m, 48H), 1.20−1.12 (t, 12H), 0.93−0.88 (m, 24H). ^{13}C NMR ($CDCl_3$, 100 MHz, δ/ppm): 142.9, 139.9, 134.2, 132.9, 128.2, 73.6, 31.9, 30.6, 29.7, 29.7, 29.6, 29.4, 29.1, 29.0, 28.9, 27.3, 26.2, 22.7, 14.1, 13.7, 10.9.

Synthesis of Terpolymers. Compounds **M1** (0.6 mmol), **M2** (0.6 mmol), and **M3** (0.6 mol) were stirred in 15 mL toluene solution under N_2 protection, followed by adding $Pd(PPh_3)_4$ (10 mg). The monomer ratios of the terpolymers were successfully controlled, depending on the initial adding amount of the reagent. The end-capping and extraction procedures followed the copolymerizing method reported in literature.[24] A yield of 72−89% of resultant was obtained.

P1: **M1** (0.1743g, 0.3 mmol), **M2** (0.1986g, 0.3 mmol), **M3** (0.6822g, 0.6 mmol), toluene (15 mL), $Pd(PPh_3)_4$ (10 mg), and P(o-toly)$_3$ (14 mg) were used, resulting in a yield of 78.0% reaction product. ^{1}H NMR($CDCl_3$, 400 Hz, δ/ppm): 9.02 (d, 1H), 7.53(t, 3H), 7.15 (d, 2H), 6.87 (d, 2H), 6.70 (d, 1H), 4.46−3.82 (m, 14H), 1.97−1.25 (m, 140H), 0.87 (s, 21H). ^{13}C NMR($CDCl_3$, 100 MHz, δ/

DOI: 10.1021/acsami.5b04697
ACS Appl. Mater. Interfaces 2015, 7, 17408−17415

ppm): 152.9, 151.1, 143.6, 129.7, 125.1, 124.7, 47.7, 31.9, 30.7, 30.5, 29.7, 29.4, 26.8, 26.2, 22.7, 14.1.

P2: **M1** (0.2614g, 0.45 mmol), **M2** (0.0993g, 0.15 mmol), **M3** (0.6822g, 0.6 mmol), toluene (15 mL), $Pd(PPh_3)_4$ (10 mg), and P(o-toly)$_3$ (14 mg), resulting in a yield of 80.4% product. ^{1}H NMR($CDCl_3$, 400 Hz, δ/ppm): 9.02 (d, 1H), 7.51−6.88 (m, 8H), 4.39−3.55 (m, 12H), 1.98−1.25 (m, 146H), 0.86 (s, 24H). ^{13}C NMR($CDCl_3$, 100 MHz, δ/ppm): 144.7, 144.0, 129.4, 129.0, 124.7, 115.5, 114.9, 31.9, 30.7, 30.6, 29.7, 29.4, 27.2, 26.9, 26.2, 26.1, 22.7, 14.1.

P3: **M1** (0.2905g, 0.5 mmol), **M2** (0.0662g, 0.1 mmol), **M3** (0.6822g, 0.6 mmol), toluene (15 mL), $Pd(PPh_3)_4$ (10 mg), and P(o-toly)$_3$ (14 mg) were used, resulting in a yield of 89.0% product. ^{1}H NMR($CDCl_3$, 400 Hz, δ/ppm): 9.03 (d, 1H), 7.51−6.67 (m, 8H), 4.31−4.02 (m, 6H), 1.93−1.25 (m, 84H), 0.87 (s, 15H). ^{13}C NMR($CDCl_3$, 100 MHz, δ/ppm): 144.6, 144.0, 142.3, 132.7, 129.4, 128.9, 125.0, 124.7, 115.5, 114.9, 47.8, 31.9, 30.6, 29.7, 29.4, 26.9, 26.2, 26.1, 22.7, 14.1.

P4: **M1** (0.3050g, 0.525 mmol), **M2** (0.0497g, 0.075 mmol), **M3** (0.6822g, 0.6 mmol), toluene (15 mL), $Pd(PPh_3)_4$ (10 mg), and P(o-toly)$_3$ (14 mg) were used, resulting in a yield of 82.3% product. ^{1}H NMR($CDCl_3$, 400 Hz, δ/ppm): 7.50−6.48 (m, 8H), 4.29−3.86 (br, 6H), 2.51−1.24 (br, 88H), 0.86 (s, 15H). ^{13}C NMR($CDCl_3$, 100 MHz, δ/ppm): 144.7, 144.0, 133.5, 132.7, 129.4, 129.0, 127.4, 125.4, 124.6, 115.4, 114.9, 47.7, 31.9, 30.7, 30.6, 29.7, 29.3, 26.9, 26.1, 22.7, 14.1.

Device Fabrication. Briefly, TiO_2 colloid was prepared by hydrothermal method, which was described in our previous work.[20,21] The TiO_2 film was spin-coated onto a FTO glass, followed by postcalcination at 450 °C for 30 min. The film was then put into the terpolymer toluene solution for 12 h. Finally, a hole transport layer PEDOT:PSS and a Pt electrode were successively deposited to form the solar cell. The photoactive area of the HSC device is about 0.25 cm^2.

3. RESULTS AND DISCUSSION

3.1. Materials Design, Synthesis, and Characterization. Scheme 1 illustrates the synthetic route of the terpolymers. Bromination of 10-hexadecyl-10H-phenothiazine with Br_2 gave **M1** in 61% yield.[35] **M2** was prepared in good yields over three steps starting from the readily available 1, 2-dialkoxy-4,5-dinitrobenzene.[36] **M3** was prepared from thiophene-3-carboxylic acid.[38] Random terpolymers **P1**−**P4** that consist of PTZ and BDT were prepared by Stille coupling polymerization, where the monomer **M3** reacted with **M1** and **M2** depending on their initial adding amounts (see Experimental Section).

All of the terpolymers dissolve well in some organic solvents such as tetrahydrofuran, toluene, and chloroform, because of their hexadecyl and didodecyl units. The weight-average molecular weight (M_w) and polydispersity index (M_w/M_n) were investigated by gel permeation chromatography (GPC). Table 1 shows that the M_n of the terpolymers ranges from 4307 to 24 738, whereas their polydispersity indices are 1.14−1.30. Moreover, TGA results reveal good thermal stability of the terpolymers, whose decomposition temperatures (5% weight loss temperature) are as high as 309−313 °C, as shown in Figure 1. These excellent properties promise this type of terpolymers to be potential candidate for optoelectronic applications.

Table 1. Molecular Weights and Thermal Parameters of Terpolymers

terpolymers	M_n[a]	M_w[a]	PDI	T_d[b] (°C)
P1	4307	5165	1.19	309
P2	20349	24349	1.19	313
P3	24738	28394	1.13	311
P4	15233	19877	1.30	311

[a]M_n, M_w, and PDI of the terpolymers obtained from GPC results. [b]Decomposition temperature.

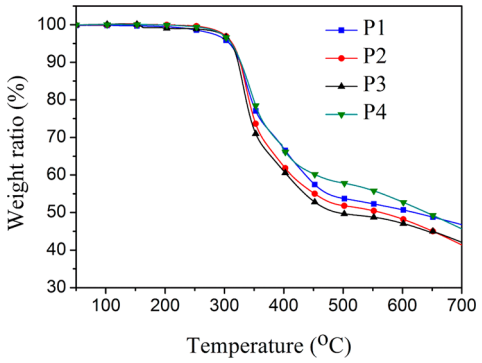

Figure 1. TGA thermograms of the terpolymers.

3.2. Electronic structure properties. Initially, the motivation of using D−A terpolymers is to match the solar light spectrum. Compared to high-performance polymers, many terpolymers possess similar or much smaller optical absorption band edges indeed, whereas their corresponding PCEs are fairly low.[39] That the energy level mismatch induces inefficient charge separation is one of the key factors accounting for the poor performances of these photovoltaic devices.[40] Besides, our recent works also demonstrate that the energy offset between the donor and acceptor plays a crucial role in the photoexcited charge transfer efficiency.[41,42] This prompts us to scrutinize the features of polymer electronic structure beyond their bandgaps.

Density functional theory (DFT) calculations were applied to demonstrate the electronic structures of these terpolymers by the DFT (B3LYP/6-31G** level) method using the Gaussian 09 program suite, conducting at lowest vertical excitation after optimizing the geometrical structures. Since the alkyl groups have little significant influence on their equilibrium geometries and the electronic behaviors, therefore we replace the long alkyl side chains with methyl for simplicity in these calculations. The electronic structures of the model compound after optimizing geometry configuration are shown in Figure 2a. As a result, the local electron density exhibits a clear "push−pull" tendency along the backbone due to the electron affinity differences between the PZT-BDT and BT-BDT blocks. On one hand, the electron density dominates the block PZT-BDT and has the tendency to delocalize onto their neighboring

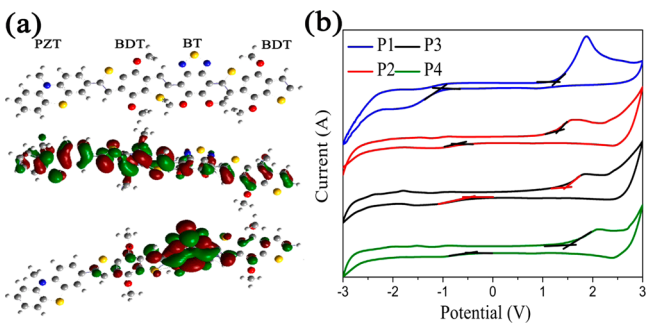

Figure 2. (a) Electronic structures of the model compound, (b) cyclic voltammogram measurements of the terpolymers.

DOI: 10.1021/acsami.5b04697
ACS Appl. Mater. Interfaces 2015, 7, 17408−17415

benzothiadiazole groups at the HOMO orbits, indicating that the π-electrons can be easily delocalized by introducing the 2D conjugated structure. On the other hand LUMO orbits are mainly localized on BT unit, which verifies its electron withdrawing behaviors. Therefore, we conclude that the PZT-BDT can play as the quasi-electron donor, whereas BT-BDT may act as the quasi-electron acceptor.

Cyclic voltammetrys (CVs) were also employed to estimate the energy levels of the polymer as shown in Figure 2b, where the redox waves are clearly revealed, implying that present terpolymers are capable of transporting the electrons as well as holes. Finally the energy levels of HOMO and LUMO can be calculated using the following formula: HOMO (or LUMO) (eV) = $-4.8 - (E_{onset} - E_{1/2})$, where $E_{1/2}$ (0.44 eV) is the potential difference between a standard ferrocene and the Ag/Ag$^+$ electrode,[43] and E_{onset} is the starting point of redox potential.[44] All the electrochemical redox parameters are summarized in Table 2. The bandgap values agree well with UV−vis results, indicating that our current works are performed on a reliable basis. The moderate D/A ratio (7:1) delivers a much deeper HOMO energy level, whereas the bandgap is almost kept unchanged, which may in turn to give relatively higher V_{oc} in solar cell devices.

Table 2. Optical Band Gaps, Electrochemical Parameters of the Terpolymers

films	E^{red}_{onset} (V)/LUMO (eV)	E^{ox}_{onset} (V)/HOMO (eV)	$E_g{}^a$ (eV)	$E_g{}^b$ (eV)
P1	−1.03/−3.33	1.21/−5.67	2.24	1.99
P2	−0.67 /−3.69	1.33/−5.69	2.00	1.96
P3	−0.49/−3.87	1.46/−5.72	1.95	1.93
P4	−0.39/−3.97	1.53/−5.89	1.92	1.89

[a]Calculated by $E_g = 1240/\lambda$, where λ is the absorption band edge of the terpolymer. [b]E_g = LUMO − HOMO.

3.3. Optical Properties. The absorption spectra of the terpolymer THF solutions are shown in Figure 3a. Each of the polymers exhibits a wide absorption band ranging from 500−650 nm, which could be assigned to the intramolecular charge-transfer (ICT) transitions between the electron-rich and the electron-deficient units, accompanied by a narrow absorption band at shorter wavelength (~425 nm) due to the transitions at higher energy region, i.e., the π−π* transitions from the heptacyclic units.[45] Compared to other polymers, **P4** revealed an identical peak at 425 nm, but a more flat absorption band with a notable red shift of the low energy absorption band edge (from 623 to 656 nm), thus leading to a narrower band gap, i.e., 1.89 eV. This suggests that the electron-donating behavior of BDT-BT that contains the electron-withdrawing BDT group is much weaker than that of the PZT-BDT moiety, leading to prominent intermolecular interactions as expected, which agrees well with DFT analysis. Besides, introducing the two electron-deficient units (PZT-BDT) gives a strong effect on lowering the bandgap of the terpolymers, i.e., from 1.99 to 1.89 eV after optimizing the ratio of the monomers. The emission spectra of the terpolymers were also investigated and are shown in Figure 3b. All of the terpolymers showed very similar emission profiles under identical excitation wavelength. A prominent peak followed by a shoulder peak was observed. The emission peaks are located at 519 nm, which is ascribed to π−π* transitions that are almost the same as each other, whereas their shoulder peaks related to ICT vary slightly. This trend is consistent with their corresponding absorption spectra. After decomposed the emission spectra into two parts, we found that the **P4** exhibited a slight redshift emission of shoulder peak, i.e., from 565 to 575 nm as compared to **P1**. Moreover, the **P4** reveals the highest ratio of integrated area of the ICT band, i.e., 0.68 as compared to the lowest 0.56 of **P1**. These results again imply that **P4** possesses strongest ICT character upon excitation, whereas **P1** bears the lowest.

3.4. Photoluminescence lifetimes of the terpolymers. Because a quasi-neutral region is included in almost all D−A terpolymers,[46] and the electric field plays a less important role in the light-absorbing material, the neutral exciton lifetime of the absorber becomes an important parameter in device performance. Long lifetime of the neutral exciton is crucial to ensure that it can diffuse to the interface of the donor and acceptor in case that the recombinations may occur. Neutral excitons that are related to ICT process can be distinguished by their spectral signatures such as stimulated emissions. Hereby, transient PL experiments with a time resolution of ~60 ps were performed on the solution of four polymers. We have chosen a suitable pump wavelength (550 nm), which allows one to selectively excite the terpolymers in the low-energy absorption band and examine the kinetics of the neutral exciton. The very low-energy excitation pulse (pump fluence <10 μJ cm^{-2}) was applied in the transient PL experiments to avoid those undesired phenomenon such as polaron pair formation or exciton annihilation. Figure 4a shows the time-resolved emission decays of the four polymers. The absence of strong oscillations in the emission decays near the band edge implies

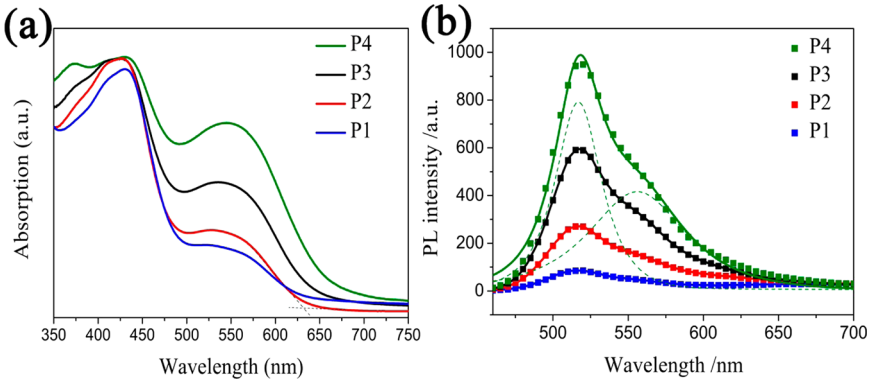

Figure 3. (a) UV−vis absorption spectra of the terpolymers; (b) photoluminescence spectra of the terpolymers, dashed lines are the decomposition of the spectra.

DOI: 10.1021/acsami.5b04697
ACS Appl. Mater. Interfaces 2015, 7, 17408−17415

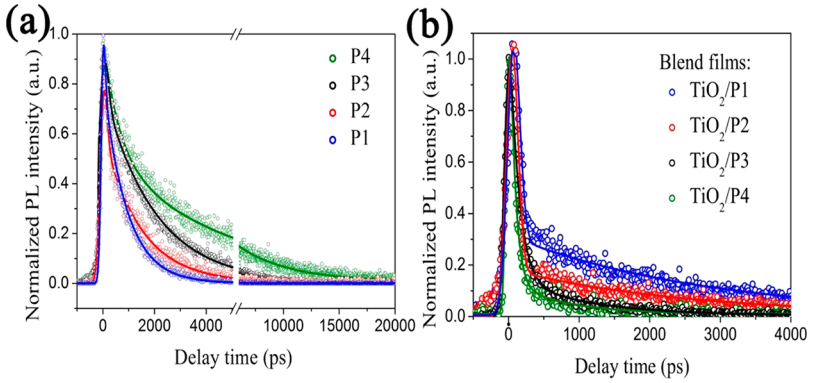

Figure 4. Time-resolved PL results of the (a) terpolymers and (b) TiO_2/terpolymer blend films.

that the emission peak decays from neutral excitations. All of the polymers exhibit almost the same profiles near the zero time delay, which is attributed to the instantaneous response of autocorrelation of laser pulse. Nevertheless, the four signals exhibit exponential decay kinetics with different lifetimes at the positive delay time. The decay kinetics is biphasic with a fast emission relaxation followed by a relatively slower relaxation. From analyzing the slope of the curves, biexponential decay kinetics is found to be satisfactory in the determination of emission lifetimes.

$$S(t) = \int_{-\infty}^{+\infty} G(\mathrm{t} - \tau)[\delta(\tau) + a_1\exp(-\tau/\tau_1) + a_2\exp(-\tau/\tau_2)]\mathrm{d}\tau \quad (1)$$

where S is the signal, G is background-free laser pulse autocorrelation function, a_1 and a_2 are the amplitude, and τ is the time constant. The average lifetimes of the emission decay can be obtained by following expression

$$\langle\tau\rangle = \frac{a_1\tau_1^2 + a_2\tau_2^2}{a_1\tau_1 + a_2\tau_2} \quad (2)$$

These decays are well-fitted with biexponential equation and the kinetic parameters are listed in Table 3. All of the terpolymers exhibit the long-lived emission decay on ns time scales. The average emissive lifetimes of the terpolymers were tested for several times, and we found that their emissive lifetimes varied clearly, depending on the ratio of the monomers. Terpolymer **P4** delivered a longest neutral exciton lifetime, i.e., 3071 ps, almost 6 times longer than that of **P1**. This suggests that the neutral exciton lifetime can be tuned effectively. The interactions between chains are changed by altering the ratio of the electron-rich and electron-deficient units, thus resulting in a variation on delocalization of the excited states and eventually the neutral exciton lifetimes.

Table 3. Kinetic Parameters Obtained from Fits to the PL Decays

kinetic parameters	a_1	a_2	τ_1 (ps)	τ_2 (ps)	$\langle\tau\rangle$ (ps)	k_{CT} ($\times 10^9$ s^{-1})
P1	0.35	0.67	116 ± 13	909 ± 5	573	1.00
TiO_2/P1	0.68	0.33	119 ± 11	1221 ± 20	349	
P2	0.34	0.70	260 ± 18	1187 ± 15	759	1.01
TiO_2/P2	0.71	0.30	112 ± 11	1621 ± 23	429	
P3	0.31	0.71	230 ± 19	1973 ± 15	1336	2.61
TiO_2/P1	0.75	0.24	135 ± 10	1421 ± 14	286	
P4	0.32	0.70	607 ± 35	4634 ± 87	3071	3.79
TiO_2/P4	0.76	0.26	155 ± 12	1129 ± 11	243	

Comparative study of the photoluminescence between the terpolymers and terpolymers interfaced with an appropriate electron-extraction layer (TiO_2) would allow us to roughly estimate the charge transfer behaviors of the BHJs by evaluating the emission quenching strengths. Figure 4b reveals that the PL intensity of the four blend films are greatly quenched after about 280 ps, indicating that these TiO_2/terpolymer blends are capable of transporting electrons/holes in an efficient way. Comparative studies on the neat terpolymers against the corresponding junctions enable us to assess the charge transfer rates in detail. The average PL lifetimes ($\tau_{\text{blend film}}$) of the blend films are obtained by fitting the transients to eq 2 and listed in Table 3. By applying the relation $k_{CT} = 1/\tau_{\text{blend film}}\text{-}1/\tau_{\text{polymer}}$,[47] the charge transfer rates k_{CT}can be estimated to be 1.00, 1.01, 2.61, and 3.79 × 10^9 s^{-1} for TiO_2/**P1**, TiO_2/**P2**, TiO_2/**P3**, and TiO_2/**P4** blends, respectively. The TiO_2/**P4** junction exhibits a much faster charge transfer rate, which is at least 3 times faster than that of the TiO_2/**P1** junction. In a short conclusion, **P4** shows the longest neutral exciton lifetime, fast charge transfer rate as well as quite small bandgap could therefore negate the undesired mechanisms such as recombination and lead to enhanced device efficiencies, provided of course a useful work for directing the charge carriers to the external circuit.

3.5. Device Performances. With a view of exploring the final photovoltaic performances of the devices with different terpolymers, we prepared the bulk-heterojuctions (BHJs) by soaking the acceptor film (TiO_2) in copolymer solution to form a donor−acceptor blend film. It can be observed from the SEM images in Figure 5a that the acceptor layer clearly reveals lots of pores, which can trap the terpolymers by physical adsorption. The side-view scanning electron microscope (SEM) images in Figure 5c, d highlight the considerable differences between the film morphologies before and after soaking processes. The pores are almost invisible in the BHJ compared to that in bare TiO_2 film. This suggests that the terpolymers penetrate well into the porous network of the TiO_2 film to form an intimate interface contact. The BHJ reveals a flat morphology, having an average film thickness of approximately 400 nm that is slightly thicker than that of bare TiO_2 as expected. The intimate contact between donor and acceptor is crucial to the efficient exiton separation, because the photoexcited exiton cannot difuse too long for polymers, usually within 12 nm.[48] HSCs based on different terpolymers were fabricated and were tested for 5 times at the same experimental conditions. The typical photocurrent−voltage (J-V) characteristics of HSCs with the

DOI: 10.1021/acsami.5b04697
ACS Appl. Mater. Interfaces 2015, 7, 17408−17415

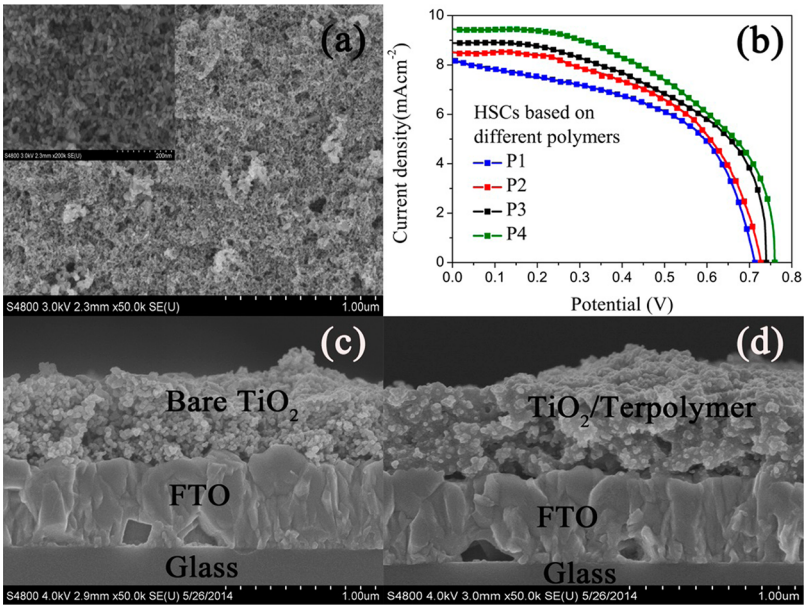

Figure 5. (a) SEM images of the TiO_2, the inset is high-magnification SEM image. (b) $J-V$ characteristic curves of TiO_2/terpolymer HSCs. Cross-sectional SEM images of bare (c) TiO_2 and (d) TiO_2/terpolymer BHJ.

four polymers were shown in Figure 5b. The statistic device parameters were listed in Table 4. The HSC with **P4** yields a remarkable η = 3.72%, J_{sc} = 9.38 mA cm^{-2}, V_{oc} = 0.76 V, and FF = 0.52, which are much higher than that of other polymers. This enhancement on one hand may be attributed to the fact that the photoactive layer **P4** has better light harvest capability than its counterparts owing to its narrower band gap, hence delivering a notable current density. On the other hand, the HOMO level of **P4** is deeper than that of other polymers, while CB energy level of acceptor remains unchanged (−4.2 eV), thus leading to a higher V_{oc} according to the relationship, from which the V_{oc} is partly governed by the CB-HOMO offset.[49] CVs results have demonstrated that **P4** have the deepest HOMO level, thus giving largest CB-HOMO offset (1.79 eV), which may be responsible for the slightly increased V_{oc}. Moreover, **P4** reveals the longest neutral exiton lifetime which guarantees the exitons have enough time to be extracted efficiently at the interface, thus leading to a notable performance.

Table 4. Photovoltaic Parameters of the HSCs

terpolymer	V_{oc} (V)	J_{sc} (mA cm^{-2})	FF	η (%)
P1	0.71 ± 0.01	8.27 ± 0.07	0.52 ± 0.01	3.06 ± 0.04
P2	0.73 ± 0.01	8.73 ± 0.18	0.51 ± 0.01	3.26 ± 0.04
P3	0.74 ± 0.01	9.03 ± 0.15	0.52 ± 0.01	3.48 ± 0.05
P4	0.76 ± 0.01	9.38 ± 0.19	0.52 ± 0.01	3.72 ± 0.09

4. CONCLUSIONS

In summary, we have synthesized random donor−acceptor copolymers via the Stille coupling reaction. The terpolymers exhibit good solubility in organic solvents, good thermal stability, broad absorption ability, and a low-lying HOMO energy level. By copolymerizing the monomers with different ratios, their band gaps and molecular energy levels are tuned simultaneously. In particular, the effects of monomer ratio on neutrual exiton times are investigated by transient PL spectroscopy. We demonstrate the PL lifetimes could be increased by optimizing the monomer ratio. In detail, **P4** exhibited the longest PL lifetime, i.e., 3071 ps, which is 5 times longer than **P1**. Besides, the TiO_2/**P4** junction exhibits prominent charge transfer ability as compared to its counterparts. The HSC based on **P4** delivers a high V_{oc} of 0.76 V and device efficiency of 3.72%, because of its lower HOMO level, smaller bandgap, longer neatrual exiton lifetime and faster charge transfer rate. Although this work is far from being optimized, and the PCE of the final device is not outstanding, these profound advantages such as deep HOMO level, ease of fabrication, and especially scalability in tuning the PL lifetimes make this terpolymer a promising candidate for robust solar cells. We expect that with further construction such as copolymerizing suitable monomers, the PL lifetime can be extended even further and ensure that the photoexcited extions have enough time to be extracted efficiently, thus achieving excellent photoelectric properties.

AUTHOR INFORMATION

Corresponding Author

*E-mail: luoxubiao@126.com.

Author Contributions

†Q.L. and X.J. contributed equally.

Notes

The authors declare no competing financial interest.

ACKNOWLEDGMENTS

We gratefully acknowledge the financial support of the Natural Science Foundation of China (61366003), Natural Science Foundation of Jiangxi Province (20151BAB212001), Science and Technology Project of the education department of Jiangxi Province, China (GJJ13474, GJJ14533).

REFERENCES

(1) Swanson, R. M. Applied Physics. Photovoltaics Power Up. *Science* **2009**, *324*, 891−892.

DOI: 10.1021/acsami.5b04697
ACS Appl. Mater. Interfaces 2015, 7, 17408−17415

(2) Lee, J.; Mubeen, S.; Hernandez-Sosa, G.; Sun, Y.; Toma, F. M.; Stucky, G. D.; Moskovits, M. High-Efficiency Panchromatic Hybrid Schottky Solar Cells. *Adv. Mater.* **2013**, *25*, 256−260.
(3) Zhou, Y.; Eck, M.; Krüger, M. Bulk-Heterojunction Hybrid Solar Cells Based on Colloidal Nanocrystals and Conjugated Polymers. *Energy Environ. Sci.* **2010**, *3*, 1851−1864.
(4) Lei, Y.; Jia, H.; He, W.; Zhang, Y.; Mi, L.; Hou, H.; Zhu, G.; Zheng, Z. Hybrid Solar Cells with Outstanding Short-Circuit Currents Based on a Room Temperature Soft-Chemical Strategy: The Case of P3HT:Ag_2S. *J. Am. Chem. Soc.* **2012**, *134*, 17392−17395.
(5) Wright, M.; Uddin, A. Organic—Inorganic Hybrid Solar Cells: A Comparative Review. *Sol. Energy Mater. Sol. Cells* **2012**, *107*, 87−111.
(6) Adikaari, A. A. D. T.; Dissanayake, D. M. N. M.; Silva, S. R. P. Hybrid Organic-Inorganic Solar Cells: Recent Developments and Outlook. *IEEE J. Sel. Top. Quantum Electron.* **2010**, *16*, 1595−1606.
(7) Chandrasekaran, J.; Nithyaprakash, D.; Ajjan, K. B.; Maruthamuthu, S.; Manoharan, D.; Kumar, S. Hybrid Solar Cell Based on Blending of Organic and Inorganic Materials—An Overview. *Renewable Sustainable Energy Rev.* **2011**, *15*, 1228−1238.
(8) Gao, F.; Ren, S.; Wang, J. The Renaissance of Hybrid Solar Cells: Progresses, Challenges, and Perspectives. *Energy Environ. Sci.* **2013**, *6*, 2020−2040.
(9) Shoaee, S.; Briscoe, J.; Durrant, J. R.; Dunn, S. Acoustic Enhancement of Polymer/ZnO Nanorod Photovoltaic Device Performance. *Adv. Mater.* **2014**, *26*, 263−268.
(10) Wang, X.; Ishwara, T.; Gong, W.; Campoy-Quiles, M.; Nelson, J.; Bradley, D. D. C. High-Performance Metal-Free Solar Cells Using Stamp Transfer Printed Vapor Phase Polymerized Poly(3,4-Ethylenedioxythiophene) Top Anodes. *Adv. Funct. Mater.* **2012**, *22*, 1454−1460.
(11) Kroon, R.; Lenes, M.; Hummelen, J. C.; Blom, P. W. M.; de Boer, B. Small Bandgap Polymers for Organic Solar Cells (Polymer Material Development in the Last 5 Years). *Polym. Rev.* **2008**, *48*, 531−582.
(12) Koppe, M.; Egelhaaf, H.-J.; Clodic, E.; Morana, M.; Lüer, L.; Troeger, A.; Sgobba, V.; Guldi, D. M.; Ameri, T.; Brabec, C. J. Charge Carrier Dynamics in a Ternary Bulk Heterojunction System Consisting of P3HT, Fullerene, and a Low Bandgap Polymer. *Adv. Energy Mater.* **2013**, *3*, 949−958.
(13) Ohkita, H.; Ito, S. Transient Absorption Spectroscopy of Polymer-Based Thin-Film Solar Cells. *Polymer* **2011**, *52*, 4397−4417.
(14) Clarke, T. M.; Durrant, J. R. Charge Photogeneration in Organic Solar Cells. *Chem. Rev.* **2010**, *110*, 6736−6767.
(15) Günes, S.; Neugebauer, H.; Sariciftci, N. S. Conjugated Polymer-Based Organic Solar Cells. *Chem. Rev.* **2007**, *107*, 1324−1338.
(16) Cook, S.; Furube, A.; Katoh, R. Analysis of the Excited States of Regioregular Polythiophene P3HT. *Energy Environ. Sci.* **2008**, *1*, 294−299.
(17) Ferreira, B.; da Silva, P. F.; Seixas de Melo, J. S.; Pina, J.; Maçanita, A. Excited-State Dynamics and Self-Organization of Poly(3-hexylthiophene) (P3HT) in Solution and Thin Films. *J. Phys. Chem. B* **2012**, *116*, 2347−2355.
(18) Kraabel, B.; Moses, D.; Heeger, A. J. Direct Observation of the Intersystem Crossing in Poly(3-octylthiophene). *J. Chem. Phys.* **1995**, *103*, 5102−5108.
(19) Greaney, M. J.; Das, S.; Webber, D. H.; Bradforth, S. E.; Brutchey, R. L. Improving Open Circuit Potential in Hybrid P3HT:CdSe Bulk Heterojunction Solar Cells via Colloidal tert-Butylthiol Ligand Exchange. *ACS Nano* **2012**, *6*, 4222−4230.
(20) Jin, X.; Li, Q.; Li, Y.; Chen, Z.; Wei, T. H.; He, X.; Sun, W. Energy Level Control: Toward an Efficient Hot Electron Transport. *Sci. Rep.* **2014**, *4*, 5983.
(21) Li, Q.; Yuan, Y.; Chen, Z.; Jin, X.; Wei, T. H.; Li, Y.; Qin, Y.; Sun, W. Core-shell Nanophosphor Architecture: Toward Efficient Energy Transport in Inorganic/Organic Hybrid Solar Cells. *ACS Appl. Mater. Interfaces* **2014**, *6*, 12798−12807.
(22) Li, W.; Roelofs, W. S.; Turbiez, M.; Wienk, M. M.; Janssen, R. A. Polymer Solar Cells with Diketopyrrolopyrrole Conjugated Polymers as the Electron Donor and Electron Acceptor. *Adv. Mater.* **2014**, *26*, 3304−3309.
(23) Henson, Z. B.; Mullen, K.; Bazan, G. C. Design Strategies for Organic Semiconductors Beyond the Molecular Formula. *Nat. Chem.* **2012**, *4*, 699−704.
(24) Peng, Q.; Liu, X.; Qin, Y.; Xu, J.; Li, M.; Dai, L. Pyrazino[2,3-g]quinoxaline-Based Conjugated Copolymers with Indolocarbazole Coplanar Moieties Designed for Efficient Photovoltaic Applications. *J. Mater. Chem.* **2011**, *21*, 7714−7722.
(25) Huo, L.; Ye, L.; Wu, Y.; Li, Z.; Guo, X.; Zhang, M.; Zhang, S.; Hou, J. Conjugated and Nonconjugated Substitution Effect on Photovoltaic Properties of Benzodifuran-Based Photovoltaic Polymers. *Macromolecules* **2012**, *45*, 6923−6929.
(26) Wang, N.; Chen, Z.; Wei, W.; Jiang, Z. Fluorinated Benzothiadiazole-Based Conjugated Polymers for High-Performance Polymer Solar Cells without any Processing Additives or Post-Treatments. *J. Am. Chem. Soc.* **2013**, *135*, 17060−17068.
(27) Kim, G.; Yeom, H. R.; Cho, S.; Seo, J. H.; Kim, J. Y.; Yang, C. Easily Attainable Phenothiazine-Based Polymers for Polymer Solar Cells: Advantage of Insertion ofS,S-dioxides into its Polymer for Inverted Structure Solar Cells. *Macromolecules* **2012**, *45*, 1847−1857.
(28) Tan, Q.; Yang, X.; Cheng, M.; Wang, H.; Wang, X.; Sun, L. Application of Small Molecule Donor Materials Based on Phenothiazine Core Unit in Bulk Heterojunction Solar Cells. *J. Phys. Chem. C* **2014**, *118*, 16851−16855.
(29) Jenekhe, S. A.; Lu, L.; Alam, M. M. New Conjugated Polymers with Donor−Acceptor Architectures: Synthesis and Photophysics of Carbazole−Quinoline and Phenothiazine−Quinoline Copolymers and Oligomers Exhibiting Large Intramolecular Charge Transfer. *Macromolecules* **2001**, *34*, 7315−7324.
(30) Stuart, A. C.; Tumbleston, J. R.; Zhou, H.; Li, W.; Liu, S.; Ade, H.; You, W. Fluorine Substituents Reduce Charge Recombination and Drive Structure and Morphology Development in Polymer Solar Cells. *J. Am. Chem. Soc.* **2013**, *135*, 1806−1815.
(31) Price, S. C.; Stuart, A. C.; Yang, L.; Zhou, H.; You, W. Fluorine Substituted Conjugated Polymer of Medium Band Gap Yields 7% Efficiency in Polymer−Fullerene Solar Cells. *J. Am. Chem. Soc.* **2011**, *133*, 4625−4631.
(32) Venkatesan, S.; Ngo, E. C.; Chen, Q.; Dubey, A.; Mohammad, L.; Adhikari, N.; Mitul, A. F.; Qiao, Q. Benzothiadiazole-Based Polymer for Single and Double Junction Solar Cells with High Open Circuit Voltage. *Nanoscale* **2014**, *6*, 7093−7100.
(33) Kang, T. E.; Cho, H.-H.; Kim, H. j.; Lee, W.; Kang, H.; Kim, B. J. Importance of Optimal Composition in Random Terpolymer-Based Polymer Solar Cells. *Macromolecules* **2013**, *46*, 6806−6813.
(34) Scaria, R.; Dhawan, S. K.; Chand, S. Synthesis of Fluorene Based Two Acceptor Random Copolymers for Organic Solar Cell Applications. *Synth. Met.* **2014**, *191*, 168−176.
(35) Qin, Y.; Li, X.; Sun, W.; Luo, X.; Li, M.; Tang, X.; Jin, X.; Xie, Y.; Ouyang, X.; Li, Q. Small Bandgap Naphthalene Diimide Copolymers for Efficient Inorganic−Organic Hybrid Solar Cells. *RSC Adv.* **2015**, *5*, 2147−2154.
(36) Wu, W.; Yang, J.; Hua, J.; Tang, J.; Zhang, L.; Long, Y.; Tian, H. Efficient and Stable Dye-Sensitized Solar Cells Based on Phenothiazine Sensitizers with Thiophene units. *J. Mater. Chem.* **2010**, *20*, 1772−1779.
(37) Bouffard, J.; Swager, T. M. Fluorescent Conjugated Polymers That Incorporate Substituted 2,1,3-Benzooxadiazole and 2,1,3-Benzothiadiazole Units. *Macromolecules* **2008**, *41*, 5559−5562.
(38) Hou, J.; Park, M.-H.; Zhang, S.; Yao, Y.; Chen, L.-M.; Li, J.-H.; Yang, Y. Bandgap and Molecular Energy Level Control of Conjugated Polymer Photovoltaic Materials Based on Benzo[1,2-b:4,5-b′]-dithiophene. *Macromolecules* **2008**, *41*, 6012−6018.
(39) Szarko, J. M.; Rolczynski, B. S.; Lou, S. J.; Xu, T.; Strzalka, J.; Marks, T. J.; Yu, L.; Chen, L. X. Photovoltaic Function and Exciton/Charge Transfer Dynamics in a Highly Efficient Semiconducting Copolymer. *Adv. Funct. Mater.* **2014**, *24*, 10−26.
(40) Yang, B.; Yuan, Y.; Sharma, P.; Poddar, S.; Korlacki, R.; Ducharme, S.; Gruverman, A.; Saraf, R.; Huang, J. Tuning the Energy

DOI: 10.1021/acsami.5b04697
ACS Appl. Mater. Interfaces 2015, 7, 17408−17415

Level Offset between Donor and Acceptor with Ferroelectric Dipole Layers for Increased Efficiency in Bilayer Organic Photovoltaic Cells. *Adv. Mater.* **2012**, *24*, 1455−1460.
(41) Jin, X.; Sun, W.; Chen, Z.; Wei, T.; Chen, C.; He, X.; Yuan, Y.; Li, Y.; Li, Q. Exciton Generation/Dissociation/Charge-Transfer Enhancement in Inorganic/Organic Hybrid Solar Cells by Robust Single Nanocrystalline LnP_xO_y (Ln = Eu, Y) doping. *ACS Appl. Mater. Interfaces* **2014**, *6*, 8771−8781.
(42) Li, Q.; Jin, X.; Yang, X.; Chen, C.; Chen, Z.; Qin, Y.; Wei, T.-h.; Sun, W. Reducing the Excess Energy Offset in Organic/Inorganic Hybrid Solar Cells: Toward Faster Electron Transfer. *Appl. Catal., B* **2015**, *162*, 524−531.
(43) Liu, Q.; Bao, X.; Wen, S.; Du, Z.; Han, L.; Zhu, D.; Chen, Y.; Sun, M.; Yang, R. Hyperconjugated Side Chained Benzodithiophene and 4,7-di-2-thienyl-2,1,3-benzothiadiazole Based Polymer for Solar Cells. *Polym. Chem.* **2014**, *5*, 2076−2082.
(44) Li, Y.; Zhong, H.; Li, R.; Zhou, Y.; Yang, C.; Li, Y. High-Yield Fabrication and Electrochemical Characterization of Tetrapodal CdSe, CdTe, and $CdSe_xTe_{1-x}$ Nanocrystals. *Adv. Funct. Mater.* **2006**, *16*, 1705−1716.
(45) Wu, J.-S.; Cheng, Y.-J.; Lin, T.-Y.; Chang, C.-Y.; Shih, P.-I.; Hsu, C.-S. Dithienocarbazole-Based Ladder-Type Heptacyclic Arenes with Silicon, Carbon, and Nitrogen Bridges: Synthesis, Molecular Properties, Field-Effect Transistors, and Photovoltaic Applications. *Adv. Funct. Mater.* **2012**, *22*, 1711−1722.
(46) Tautz, R.; Da Como, E.; Wiebeler, C.; Soavi, G.; Dumsch, I.; Frohlich, N.; Grancini, G.; Allard, S.; Scherf, U.; Cerullo, G.; Schumacher, S.; Feldmann, J. Charge Photogeneration in Donor-Acceptor Conjugated Materials: Influence of Excess Excitation Energy and Chain Length. *J. Am. Chem. Soc.* **2013**, *135*, 4282−4290.
(47) Xing, G.; Mathews, N.; Sun, S.; Lim, S. S.; Lam, Y. M.; Gratzel, M.; Mhaisalkar, S.; Sum, T. C. Long-Range Balanced Electron- and Hole-Transport Lengths in Organic-Inorganic $CH_3NH_3PbI_3$. *Science* **2013**, *342*, 344−347.
(48) Shaw, P. E.; Ruseckas, A.; Samuel, I. D. W. Exciton Diffusion Measurements in Poly(3-hexylthiophene). *Adv. Mater.* **2008**, *20*, 3516−3520.
(49) Scharber, M. C.; Mühlbacher, D.; Koppe, M.; Denk, P.; Waldauf, C.; Heeger, A. J.; Brabec, C. J. Design Rules for Donors in Bulk-Heterojunction Solar Cells—Towards 10% Energy-Conversion Efficiency. *Adv. Mater.* **2006**, *18*, 789−794.

DOI: 10.1021/acsami.5b04697
ACS Appl. Mater. Interfaces 2015, 7, 17408−17415